Numerical Simulation of Natural Convection in a Solar Chimney

Tayebi Tahar*‡, Djezzar Mahfoud*

*Energy Physics Laboratory, Department of Physics, Faculty of Science, Mentouri Constantine University

tahartayebi@gmail.com, mdjezzar@yahoo.fr

‡ Corresponding Author; Tayebi Tahar, Energy Physics Laboratory, Department of Physics, Faculty of Science, Mentouri Constantine University, Constantine, Algeria, tahartayebi@gmail.com

Abstract- This paper summarizes a numerical study of natural convection in a solar chimney. The Transported fluid is the air (Pr=0.702), it is considered as a Newtonian and incompressible fluid, by using the Boussinesq approximation, the governing equations are taken to be in the vorticity-stream function formulation in hyperbolic coordinates. For heating conditions we suppose an isothermal walls of the collector (T_h for the ground and T_c for the roof, with $T_h>T_c$). Solution of the defined equations has been done with numerical control volume method. We examined the effect of the system geometry on the natural convection phenomenon in the solar chimney. Finally, the simulation results have been given as airflows and temperature patterns.

Keywords- Solar chimney, Natural convection, Renewable energy, Vorticity-Stream function formulation.

1. Introduction

The solar chimney power plant system is a natural driving power generating system. It can convert solar energy first into thermal energy then into kinetic energy finally into electrical power.

The solar chimney concept was originally proposed by Professor Schlaich of Stuttgart in the late 1970s [1]. Less than 4 years after he presented his ideas at a conference, construction on a pilot plant began in Manzanares, Spain, as a result of a joint venture between the German government and a Spanish utility. A 36 kW pilot plant was built, which produced electricity for 7 years, thus proving the efficiency and reliability of this novel technology. The chimney tower was 194.6m high, and the collector had a radius of 122m. Fundamental investigations for the Spanish system were reported by Haaf et al. [2] in which a brief discussion of the energy balance, design criteria, and cost analysis were presented. Efforts were focused essentially on analyzing performances and cost of solar chimney. Bernardes et al. [3] presented a theoretical analysis of a solar chimney, operating on natural laminar convection in steady state. In order to predict thermo-hydrodynamic behavior of air, temperature conditions were imposed on entrance, so as to guarantee steady laminar flow along the device. The mathematical model was analyzed by the method of Finite volumes in generalized coordinates. Velocity field and temperature distribution in the flow were obtained under imposed thermal conditions. Von Backström and Fluri [4] investigated analytically the validity and applicability of the assumption that, for maximum fluid power. Von Backström and Gannon [5] were interested mainly in a one-dimensional compressible flow for the thermodynamic variable as dependence on chimney height, wall friction, additional losses, internal drag and area exchange. Pretorius and Kröger [6] evaluated the influence of a developed convective heat transfer equation, more accurate turbine inlet loss coefficient, quality collector roof glass and various types of soil on the performance of a large scale solar chimney power plant. Ming et al. [7] presented a mathematical model to evaluate the relative static pressure and driving force of the solar chimney power plant system and verified the model with numerical simulations. Maia et al. [8] presented a theoretical analysis of a turbulent flow inside a solar chimney. They showed that the most important physical elements in a solar chimney system are the tower dimensions as they cause the most significant variation in the flow behavior. An increase in the height and in the diameter of the tower produces an increase in the mass flow rate and a decrease in the flow

temperature. Pastohr et al. [9] presented a numerical simulation result in which the storage layer was regarded as solid. In their paper, conjugate numerical simulations of the energy storage layer, the collector and the chimney have been conducted, and the characteristics of the heat storage system, and the flow and heat transfer in the whole system have been studied. Zhou et al. [10] have performed an experimental study in a solar chimney. A pilot experimental solar chimney power setup consisting of an air collector of 10 m in diameter and an 8 m tall chimney was built. The authors noted that the temperature difference between the collector outlet temperature and the one of the ambient usually might reach as much as 24.1 8 °C, which generates the driving force of the air flow in the setup. Their data analysis showed an air temperature inversion in the latter chimney after sunrise and this is due to the increase of solar radiation from the minimum. The phenomenon clears up once a driving force is generated by a temperature high enough to overcome it. T. Chergui et al [11] presented a study considers the heat transfer process and the fluid flow in the collector and the chimney under some imposed operational conditions, the temperature difference through the Rayleigh number, the velocity field and the temperature distribution, through the system, are evaluated. Results showed local flow characteristics and it appears that for most Rayleigh numbers, the flow seems laminar except for Raleigh number of 108 where there are some disturbances.

The present study is to examine the effects of pertinent parameters such as Rayleigh number and the geometry of the system on the flows characteristics in solar chimney power plants, by solving the mathematical model represented by the Navier-Stokese quations, continuity and energy equations in hyperbolic coordinates and dimensionless form, using a numerical code (algorithm) based on finite volume method.

2. Problem formulation and basic equations

We consider a solar chimney which contains an incompressible fluid (air). The roof and ground surface create a vertical temperature gradient (active walls) (Fig.1).

The physical properties of the fluid are constant, apart from the density ρ whose variations are at the origin of the natural convection. Viscous dissipation is neglected, just as the radiation (emissive properties of the two walls being neglected). We admit that the problem is bidimensionnal, permanent and laminar.
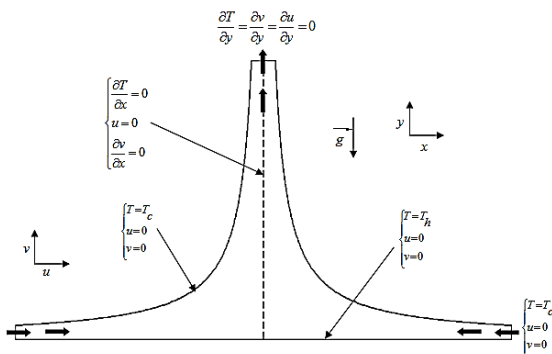

Fig. 1. Problem study and boundary conditions

The laminar natural convection equations within the framework of the Boussinesq approximation are written:

$$\frac{\partial u}{\partial x} + \frac{\partial v}{\partial y} = 0 \tag{1}$$

$$u\frac{\partial \omega}{\partial x} + v\frac{\partial \omega}{\partial y} = \frac{\partial T}{\partial x}(g\beta) + \upsilon\left(\frac{\partial^2 \omega}{\partial x^2} + \frac{\partial^2 \omega}{\partial y^2}\right) \tag{2}$$

$$u\frac{\partial T}{\partial x} + v\frac{\partial T}{\partial y} = \frac{\lambda}{\rho Cp}\left(\frac{\partial^2 T}{\partial x^2} + \frac{\partial^2 T}{\partial y^2}\right) \tag{3}$$

It is convenient to define a reference frame such as the limits of the system result in constant values of the coordinates. The passage of the cartesian coordinates (x, y) to the hyperbolic coordinates (η, θ) is obtained by the following relations:

$$\left.\begin{aligned} x &= \sqrt{\frac{r+\eta}{2}} \\ y &= \sqrt{\frac{r-\eta}{2}} \end{aligned}\right\} \tag{4}$$

With:

$$r = \sqrt{\eta^2 + \theta^2} \tag{5}$$

The metric coefficients in hyperbolic coordinates are given by:

$$h_1 = h_2 = 2\sqrt{r} \quad \text{and} \quad h3=1$$

Equations (1), (2) and (3) written then respectively:

$$\frac{\partial}{\partial \eta}(hV_\eta) + \frac{\partial}{\partial \theta}(hV_\theta) = 0 \tag{6}$$

$$V_\eta\frac{\partial T}{\partial \eta} + V_\theta\frac{\partial T}{\partial \theta} = \frac{1}{h}\frac{\lambda}{\rho Cp}\left(\frac{\partial^2 T}{\partial \eta^2} + \frac{\partial^2 T}{\partial \theta^2}\right) \tag{7}$$

$$\frac{V_\eta}{h}\frac{\partial \omega}{\partial \eta} + \frac{V_\theta}{h}\frac{\partial \omega}{\partial \theta} = \frac{\upsilon}{h^2}\left(\frac{\partial^2 \omega}{\partial \eta^2} + \frac{\partial^2 \omega}{\partial \theta^2}\right) +$$
$$\frac{g\beta}{h}\left(\sqrt{\frac{r+\eta}{2r}}\frac{\partial T}{\partial \eta} + \sqrt{\frac{r-\eta}{2r}}\frac{\partial T}{\partial \theta}\right) \tag{8}$$

The equation for the stream function:

$$\omega = -\frac{1}{h^2}\left(\frac{\partial^2 \psi}{\partial \eta^2} + \frac{\partial^2 \psi}{\partial \theta^2}\right) \tag{9}$$

The quantities characteristic used for the dimensionless problem are the $\Delta T = T_h - T_c$ between The roof and ground surface, the metric coefficients in hyperbolic coordinates (h) as reference length and the thermal diffusivity of fluid α as characteristic velocity. The dimensionless mathematical model obtained is:

$$\omega^* = -\frac{1}{h^2}\left(\frac{\partial^2 \psi^*}{\partial \eta^2} + \frac{\partial^2 \psi^*}{\partial \theta^2}\right) \qquad (10)$$

$$V_\eta^* \frac{\partial \omega^*}{\partial \eta} + V_\theta^* \frac{\partial \omega^*}{\partial \theta} = \frac{\Pr}{H}\left(\frac{\partial^2 \omega^*}{\partial \eta^2} + \frac{\partial^2 \omega^*}{\partial \theta^2}\right)$$
$$+ Ra\,\Pr\left(\sqrt{\frac{r+\eta}{2r}}\frac{\partial T^*}{\partial \eta} + \sqrt{\frac{r-\eta}{2r}}\frac{\partial T^*}{\partial \theta}\right) \qquad (11)$$

$$V_\eta^* \frac{\partial T^*}{\partial \eta} + V_\theta^* \frac{\partial T^*}{\partial \theta} = \frac{1}{H}\frac{\lambda}{\rho C p}\left(\frac{\partial^2 T^*}{\partial \eta^2} + \frac{\partial^2 T^*}{\partial \theta^2}\right) \qquad (12)$$

Where:

$$V_\eta^* = \frac{1}{H}\frac{\partial \psi^*}{\partial \theta}; V_\theta^* = -\frac{1}{H}\frac{\partial \psi^*}{\partial \eta} \qquad (13)$$

The boundary conditions are the following ones:

- *The roof of the collector*

$$V_\eta^* = V_\theta^* = 0 \text{ and } T^* = 0 \qquad (14)$$

- *The axis of symmetry*

$$\frac{\partial V_\eta^*}{\partial \theta} = 0; V_\theta^* = 0 \text{ and } \frac{\partial T^*}{\partial \theta} = 0 \qquad (15)$$

- *The ground*

$$V_\eta^* = V_\theta^* = 0 \text{ and } T^* = 1 \qquad (16)$$

- *Collector inlet*

$$V_\eta^* = V_\theta^* = 0 \text{ and } T^* = 0 \qquad (17)$$

- *Chimney outlet*

$$\frac{\partial V_\eta^*}{\partial \eta} = \frac{\partial V_\theta^*}{\partial \eta} = 0, \quad \frac{\partial T^*}{\partial \eta} = 0 \qquad (18)$$

3. Numerical Method

To solve this system of equations with associated boundary conditions equations, we consider a numerical solution by the method of finite volumes, presented by Patankar [12]. Fig.2 shows the physical domain and the computational domain.

The power law scheme was used for the discretization. The iterative method used for the numerical solution of algebraic system of equations is the Gauss-Seidel, with an under-relaxation process.
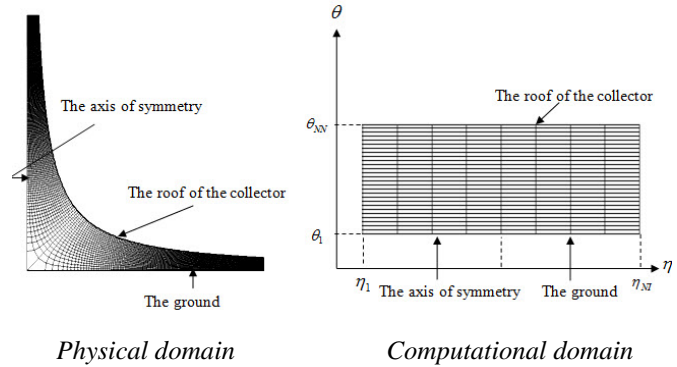

Physical domain　　　　*Computational domain*

Fig. 2. Physical domain and computational domain

4. Results and Discussion

For the validation of the computational problem, we compared our results with those of literature: The numerical simulation of transient mixed convection in a cylindrical cavity for different flow regime of A. Bouhdjar et al [13], and the study of W. Aung et al [14]. For more details concerning this question, reading the study of T. Chergui et al [11].

The grid dependence has been investigated using different mesh sizes before settling to a mesh size of (350 x 22).

Our objective is to analyze the effect of geometry on heat transfer and flow of air into the chimney. For this reason, we presented the isotherms and streamlines in two different geometries for three different Rayleigh numbers.
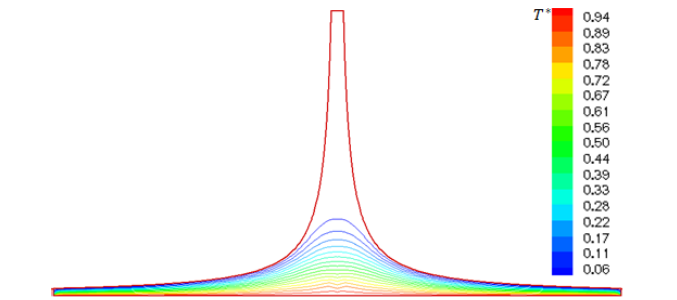

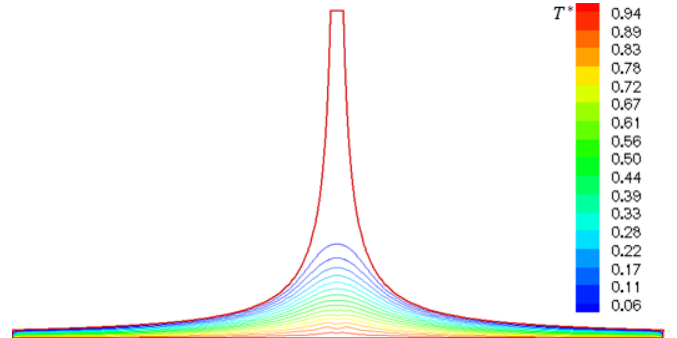**Fig. 3.** Isothermal lines for the first geometry and Ra=10^3

Fig. 4. Isothermal lines for the first geometry and Ra=10^4
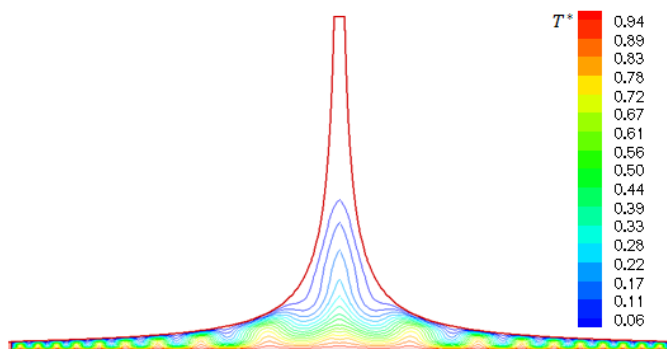
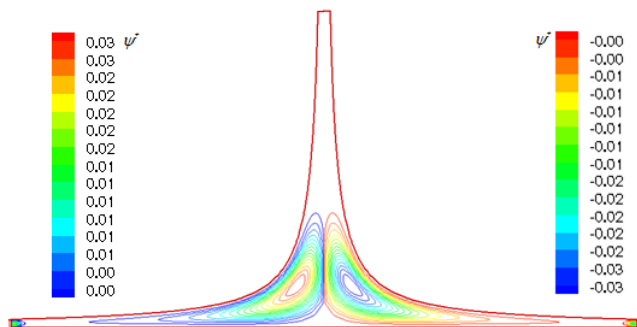**Fig. 5.** Isothermal lines for the first geometry and Ra=10^5

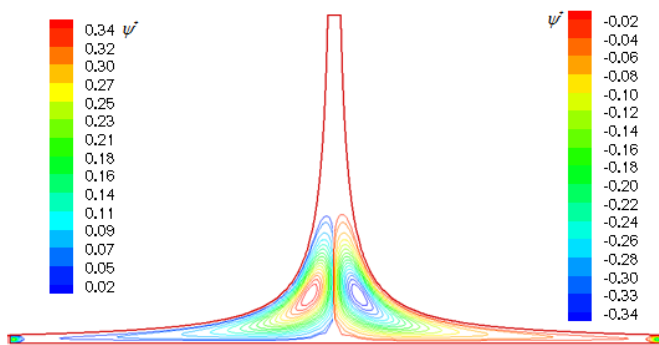**Fig. 6.** Streamlines for the first geometry and Ra=10^3

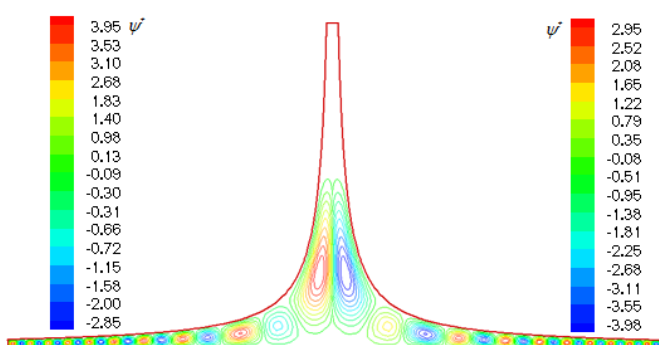**Fig. 7.** Streamlines for the first geometry and Ra=10^4

Fig. 8. Streamlines for the first geometry and Ra=10^5

Figs.3-5 show the dimensionless isothermal lines for the first geometry and for Rayleigh numbers equal to 10^3, 10^4 and 10^5 respectively. When the Rayleigh number is weak, as being lower or equal to 10^4, the heat transfer is essentially conductive, so the isotherms have the same form as the walls and the maximum temperature is located near the ground in the collector due to heat transfer exchange between this surface and the airflow beneath the cover. For a Rayleigh

number 10^5 swirls in isothermal lines are also observed in the collector area.

Figs.6-8 represent the streamlines for the first geometry and for different Rayleigh number values. For Ra = 10^3 and 10^4, we note the presence of two counter rotating vortices in the center of the collector because of the symmetrical structure of the chimney favoring the upward flow and two vortices are smaller in size at the inlet of the chimney (the particles of the fluid move upwards, under the action of gravity forces, along the hot wall and go down near to the cold wall).

For Ra = 10^5, the flow is characterized by a set of counter rotating cells (secondary cells) along the collector, and the two cells in the center move up the chimney. The streamlines values show an appreciable increase in the flow. This means that the transfer is done primarily by convection and predominates on the conduction.

When the distance between the ground and the roof is increased (second geometry), swirls was observed in the collector for a Rayleigh number is 10^4 and 10^5 (Figs.9-11), the flow which is going up on the side of ground and going down on the side of roof, becomes intense and the natural convection is dominant.

In the second geometry (Figs.12-14), the counter rotating vortices appear for Ra = 10^4 and the two vortices of the center become greatest and move up the chimney. By increasing the number of Rayleigh the vortices turn faster and the convection becomes more important.
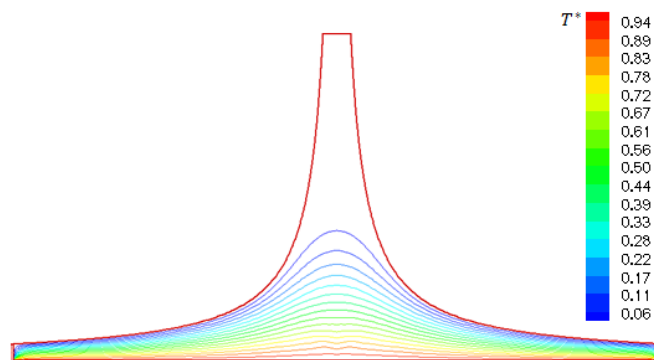

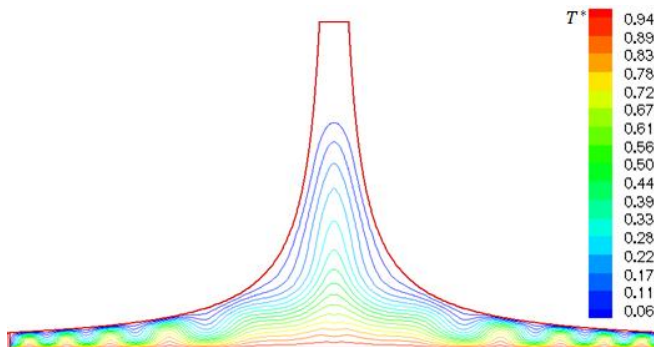**Fig. 9.** Isothermal lines for the second geometry and Ra=10^3

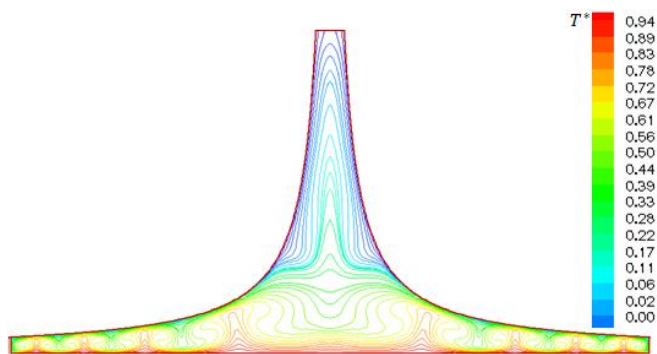**Fig. 10.** Isothermal lines for the second geometry and Ra=10^4

Fig. 11. Isothermal lines for the second geometry and Ra=10^5
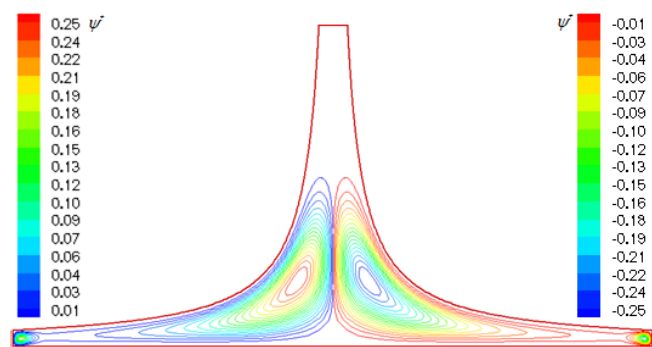

Fig. 12. Streamlines for the second geometry and Ra=10^3
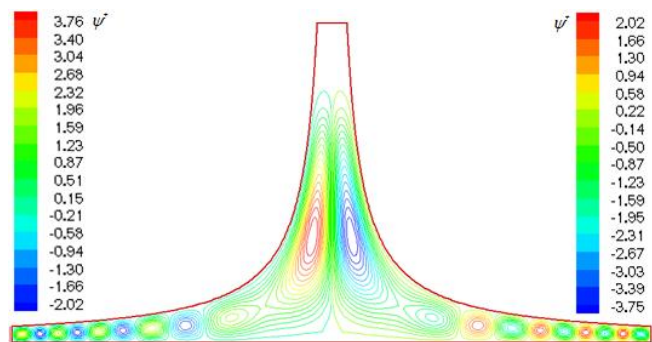

Fig. 13. Streamlines for the second geometry and Ra=10^4
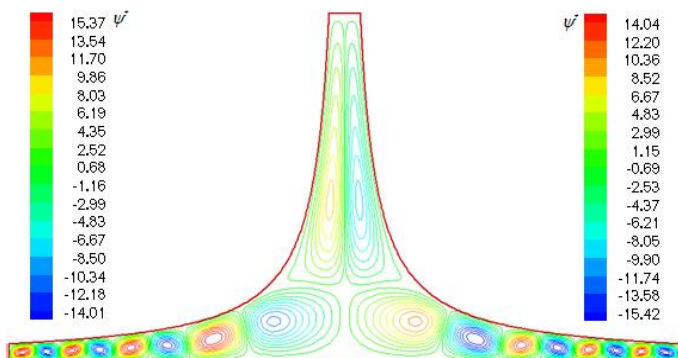

Fig. 14. Streamlines for the second geometry and Ra=10^5

Figs.15-16 illustrate the dimensionless velocity field for the first and second geometry and for Rayleigh 10^4. It should be note that its magnitude for the second geometry is higher than the one calculated in the first geometry and always its maximum is located approximately at the inlet of the chimney as it is reported in literature [9], [11] and [13]. For the region of curved junction and the inlet of the collector

different zones of flow recirculation can be observed due to instability of airflow in these areas for the first geometry and a large zone of flow recirculation inverted located below the curved wall for the second geometry.
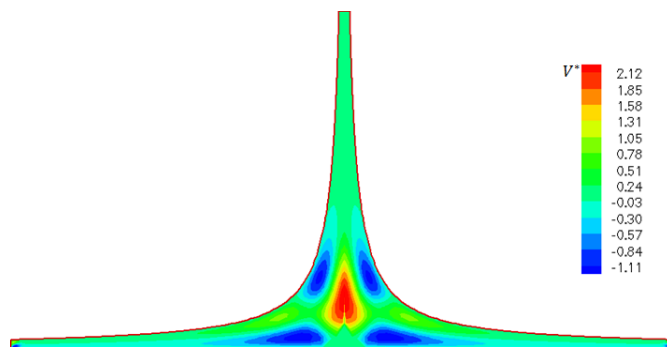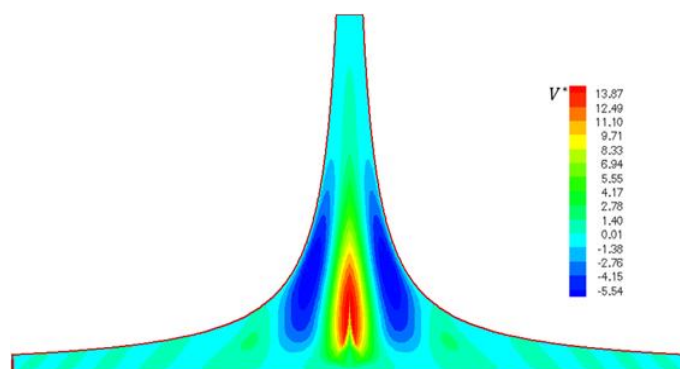

Fig. 15. Velocity field the first geometry and Ra=10^4

Fig. 16. Velocity field for the second geometry and Ra=10^4

5. Conclusion

In this paper a thermo-hydrodynamic analysis for air motion in natural convection, laminar flow and steady state with the vorticity-stream function formulation is presented for a solar chimney with prescribed boundary conditions. A validated computer program was adapted to the solar chimney configuration to solve the governing equations, which uses the method of finite volumes. We examined the effect of the system geometry on the convective mode. We considered two different geometries of the system. The simulations were executed from three values of Rayleigh number: Ra=10^3, Ra=10^4 and Ra=10^5.

Results showed that the natural convection (airflow) increases with increase in the gap (the distance) between ground and roof of the collector. It has also been found that the airflow also increases with increase the Rayleigh number.

This result will let the solar chimney designer correctly locate the turbine in the solar chimney power plant.

References

[1] J. Schlaich, The Solar Chimney: Electricity from the Sun, Edition Axel Menges, Stuttgart, Germany, 1995.

[2] W. Haaf, K. Friedrich, G. Mayer, J. Schlaich, Solar chimneys, Part I: principle and construction of the pilot

plant in Manzanares, International Journal of Solar Energy 2 (1983) 3-20.

[3] MA. Bernardes, S. dos, RM. Valle, MFB.Cortez, Numerical analysis of natural laminar convection in a radial solar heater, International Journal of Thermal Science 38 (1999) 42-50.

[4] TW. Von Backström, TP. Fluri, Maximum fluid power condition in solar chimney power plants-an analytical approach, Solar Energy 80 (2006) 1417-1423.

[5] T.W. Von Backstrom, A.J. Cannon, Compressible flow through solar power plant chimneys, Journal of Solar Energy Engineering 122 (2000) 138-145.

[6] JP. Pretorius, DG. Kröger, Critical evaluation of solar chimney power plant performance, Solar Energy 80 (2006) 535-544.

[7] TZ. Ming, W. Liu, GL. Xu, AW. Fan, A study of the solar chimney power plant systems. Journal of Engineering Thermodynamics. 3 (2006) 505-517.

[8] CB. Maia, AG. Ferreira, RM. Valle, MFB. Cortez, Theoretical evaluation of the influence of geometric parameters and materials on the behavior of the air flow in a solar chimney, Computers and Fluids. 38 (2009) 625-36.

[9] H. Pastohr, O. Kornadt, K. Gurlebeck, Numerical and analytical calculations of the temperature and flow field in the upwind power plant, International Journal of Energy Research. 28 (2004) 495-510.

[10] X. Zhou, J. Yang, B. Xiao, G. Hou, Experimental study of temperature field in a solar chimney power setup, Applied Thermal Engineering. 27 (2007) 2044-50.

[11] Toufik Chergui, Salah Larbi, Amor Bouhdjar. Thermo-hydrodynamic aspect analysis of flows in solar chimney power plants-A case study Renewable and Sustainable Energy Reviews 14 (2010) 1410-1418.

[12] S.V. Patankar, Numerical heat transfer and fluid flow, Hemisphere, Washington, D.C, 1980.

[13] A. Bouhdjar, A. Harhad, A. Benkhelifa, Numerical simulation of transient mixed convection in a cylindrical cavity, Numerical Heat Transfer 31 (1996) 305-324.

[14] W. Aung, L.S. Fletcher, V. Sernas, Development of laminar free convection between vertical flat plates with asymmetric heating, Int. J. Heat Mass Trans. 15 (1972) 2293-2308.

Symbols

C_p	: Specific heat at constant pressure, $J\ kg^{-1}\ K^{-1}$;
H	: Metric coefficient, m;
H	: Dimensionless metric coefficient;
P_r	: Prandtl number;
Ra	: Rayleigh number;
T	: Fluid's temperature, K;
T_h	: Temperature of the ground, K;
T_c	: Temperature of the roof, K;
ΔT	: Temperature difference between the inner and the outer wall, $\Delta T = T_h - T_c$, K;
u , v	: Velocities components according to coordinates x and y, $m\ s^{-1}$;
$V_\eta,\ V_\theta$	: Velocities components according to coordinates η and θ, $m\ s^{-1}$;
x, y	: Cartesian coordinates, m;

Greek symbols

β	: Thermal expansion coefficient, K^{-1};
λ	: Thermal conductivity, $W.m^{-1}\ K^{-1}$;
υ	: Kinematic viscosity, $m^2\ s^{-1}$;
ρ	: Density, $kg.m^{-3}$;
η, θ	: Hyperbolic coordinates;
ψ	: Stream function, $m^2\ s^{-1}$;
ω	: Vorticity ,s^{-1};

Subscripts

h	: Hot
c	: Cold
$*$	: Dimensionless parameters